J. Fluid Mech. (1983), *vol.* 127, *pp.* 103–121
Printed in Great Britain

Bubbles, breaking waves and hyperbolic jets at a free surface

By M. S. LONGUET-HIGGINS

Department of Applied Mathematics and Theoretical Physics, Silver Street, Cambridge, and Institute of Oceanographic Sciences, Wormley, Surrey

(Received 7 May 1982)

Experiments have shown that bubbles approaching an air–water interface give rise to axisymmetric jets projected upwards into the air. Similar jets occur during the collapse of cavitation bubbles near a solid surface. In this paper we show that such jets are well modelled by a Dirichlet hyperboloid, a hyperbolic form of the better-known ellipsoid. The vertex angle of the hyperboloid is calculated as a function of time and found to agree with the observations of Blake & Gibson (1981) and others.

The jet is initiated, according to this model, when the vertex angle passes through $2\arctan\sqrt{2}$, or 109·47°, at which instant the fluid accelerations become large. This compares with a vertical angle of 90° in the corresponding two-dimensional flow.

Further experiments demonstrate that an axisymmetric standing wave, when driven beyond its maximum amplitude, can break by throwing up a jet of the same hyperbolic form. Hyperbolic jets may occur commonly in free-surface flows.

1. Introduction

In a recent paper Blake & Gibson (1981) studied the growth and collapse of vapour bubbles close to a free surface, both numerically and experimentally. One of their experiments is reproduced, in modified form, in figure 1. As the bubble rises and expands it can be seen to raise and accelerate a thin layer of fluid in the form of a spherical dome. Then (starting at about frame no. 30) there emerges a remarkable jet rising from the dome along the axis of symmetry. The jet ultimately approximates a circular cone with diminishing vertex angle. Such a phenomenon is clearly of environmental interest for transfer of water droplets, salt nuclei and organic particles from the ocean to the atmosphere by bursting bubbles (see Blanchard & Woodcock 1980). As indicated by Blake & Gibson, similar jets issuing from the interior surface of a cavitation bubble near a solid surface, and directed towards the surface, are probably responsible for much of the damage to propellers and other fast-driven hydraulic machinery.

The numerical calculations described by Blake & Gibson agree with their observations as far as the initial formation of the jet. However, the mechanism still appears somewhat mysterious. In the present paper we propose an *analytic* model for the development of the jet. The model is in fact a hyperbolic form of the flow known in astrophysics as a Dirichlet ellipsoid, and described for example in Lamb (1932). The hyperbolic form, however, does not appear to have been seriously considered, perhaps on account of the infinite masses involved, and certain singularities in the time dependence, described below. A two-dimensional hyperbolic form has been studied by Longuet-Higgins (1972, 1976) in connection with the breaking of surface waves, and generalized in more recent papers (1980, 1982).

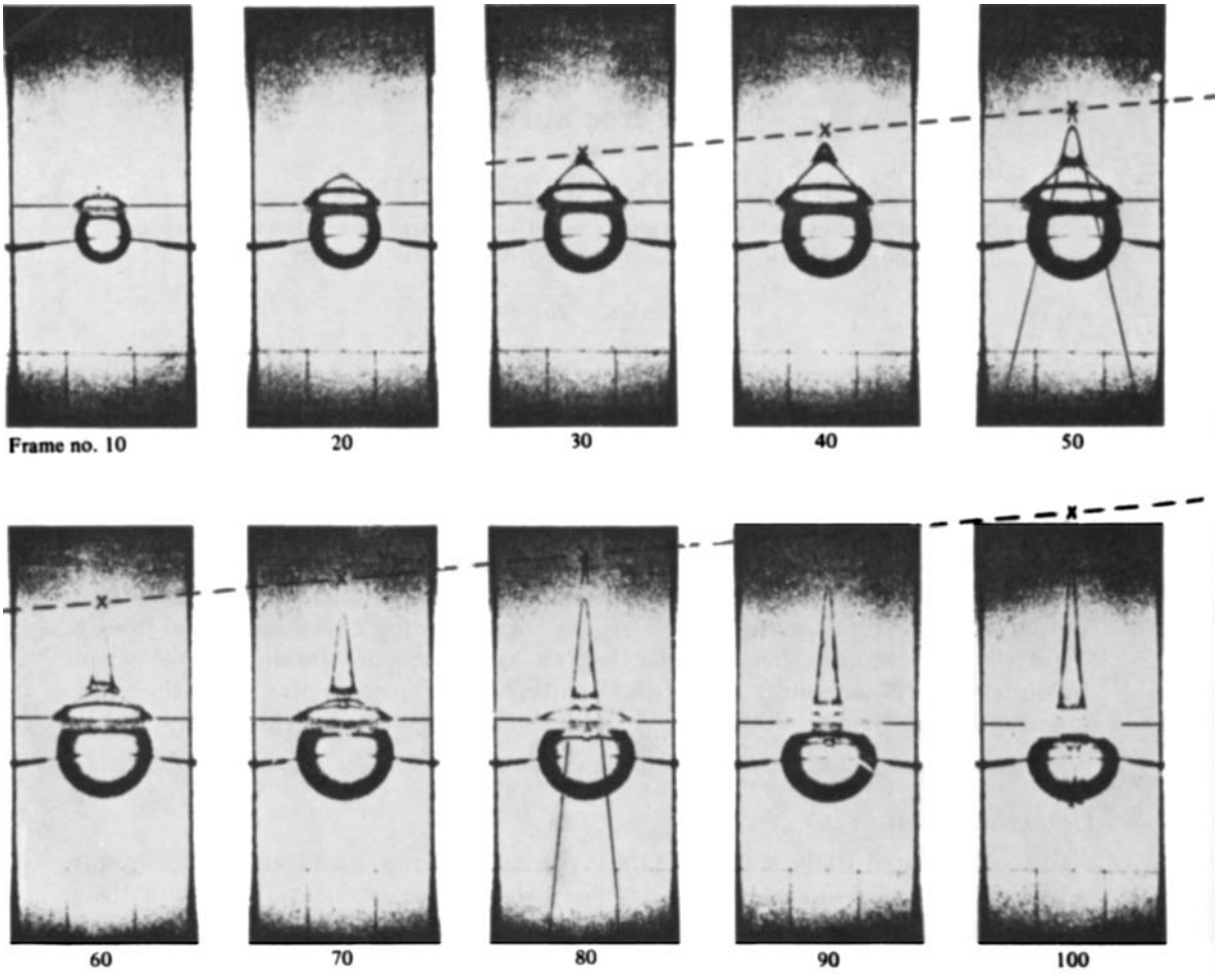

FIGURE 1. Jet produced by a gas bubble approaching a free surface (after Blake & Gibson 1981). The dashed line represents the trajectory of the assumed centre of the hyperboloid.

The theory for the three-dimensional hyperboloid is given below in §2, and the case of axial symmetry is discussed in detail in §3. One special feature of the flow is the occurrence of a 'jolt', or local infinity in the acceleration when the vertex angle of the hyperboloid equals $2\arctan\sqrt{2}$, or 109·5°. This in fact corresponds to the initiation of the jet. A comparison with Blake & Gibson's observations follows in §4, with reasonable agreement (see figure 4).

The degree of correspondence between the observations and this simple theoretical model prompted the author to enquire whether a similar flow might be observed in other situations. One example that came to mind was the jet thrown up by a standing water wave when excited by a vertical or horizontal oscillation of the container (Faraday 1831). In §6 we describe a simple experiment which in effect verifies that these jets are, in suitable circumstances, well described by the same theory.

In the appendix we enquire further into the initial 'jolt' and give a physical explanation for it. Finally, in §7 we summarize the conclusions and note possible implications for the modelling of a breaking wave.

2. The Dirichlet hyperboloids

The theory for Dirichlets' *ellipsoids* (see Dirichlet 1860) is given in Lamb (1932, §382), where it is generalized to cover both self-gravitation and rotation of the fluid as a whole. For convenience we give here an alternative derivation for the *hyperboloids* in the simplest situation, that is without rotation or self-gravitation.

The fluid is assumed inviscid and incompressible and the flow irrotational. The velocity potential, relative to rectangular coordinates (x, y, z) is taken to be of the form

$$\phi = \frac{1}{2}\left(\frac{\dot{a}}{a}x^2 + \frac{\dot{b}}{b}y^2 + \frac{\dot{c}}{c}z^2\right), \tag{2.1}$$

where a, b, c are functions of the time t only, and a dot ($\dot{}$) denotes time-differentiation. Equation (2.1) represents, in fact, the most general expression for a pure straining flow that is symmetric in regard to the three coordinate planes. The velocity vector is

$$\nabla\phi = \left(\frac{\dot{a}}{a}x, \frac{\dot{b}}{b}y, \frac{\dot{c}}{c}z\right), \tag{2.2}$$

and by continuity we have

$$\frac{\dot{a}}{a} + \frac{\dot{b}}{b} + \frac{\dot{c}}{c} = 0, \tag{2.3}$$

so that

$$abc = 2L^3, \tag{2.4}$$

is a constant of the motion.

The fluid being assumed homogeneous and of unit density and gravity negligible,† the pressure p at any point is given by

$$-2p = 2\phi_t + (\nabla\phi)^2 + F(t) = \left(\frac{\ddot{a}}{a}x^2 + \frac{\ddot{b}}{b}y^2 + \frac{\ddot{c}}{c}z^2\right) + F. \tag{2.5}$$

Hence also

$$-2\frac{Dp}{Dt} \equiv \left(\frac{\partial}{\partial t} + \nabla\phi\,.\,\nabla\right)(-2p) = \frac{a\ddot{a}+\dot{a}\dot{a}}{a^2}x^2 + \frac{b\ddot{b}+\dot{b}\dot{b}}{b^2}y^2 + \frac{c\ddot{c}+\dot{c}\dot{c}}{c^2}z^2 + \dot{F}. \tag{2.6}$$

Surface tension being also neglected, we may take as boundary conditions that both p and Dp/Dt vanish on the same surface (cf. Longuet-Higgins 1972, 1976). Thus the coefficients of corresponding terms in (2.5) and (2.6) must be in proportion. Hence

$$\frac{\dddot{a}}{\ddot{a}} + \frac{\dot{a}}{a} = \frac{\dddot{b}}{\ddot{b}} + \frac{\dot{b}}{b} = \frac{\dddot{c}}{\ddot{c}} + \frac{\dot{c}}{c} = \frac{\dot{F}}{F}, \tag{2.7}$$

and on integration

$$a\ddot{a} = K_1 F, \quad b\ddot{b} = K_2 F, \quad c\ddot{c} = K_3 F, \tag{2.8}$$

where the K_i are constants. A change in scale of a, b or c does not alter the velocity potential ϕ, so without loss of generality we may take $K_1 = -1$, $K_2 = K_3 = 1$. Then from (2.8)

$$a\ddot{a} = -b\ddot{b} = -c\ddot{c} = -F, \tag{2.9}$$

and by (2.5) the free surface $p = 0$ becomes simply

$$\frac{x^2}{a^2} - \frac{y^2}{b^2} - \frac{z^2}{c^2} = 1, \tag{2.10}$$

a hyperboloid with semi-axes a, b and c. Moreover, the continuity condition (2.3) can be written

$$\dot{a}\ddot{a} - \dot{b}\ddot{b} - \dot{c}\ddot{c} = 0, \tag{2.11}$$

† Alternatively, the flow may be viewed in a free-fall reference frame.

so that an integration $$\dot{a}^2-\dot{b}^2-\dot{c}^2 = U^2, \tag{2.12}$$

a second constant. When a, b and c have been determined as functions of t, then F is given by (2.9).

In two special cases the equations can be integrated completely.

Two-dimensional flow. This corresponds to the limit

$$\dot{c} \to 0, \quad \frac{z}{c} \to 0, \quad \frac{2L^3}{c} = l^2 < \infty. \tag{2.13}$$

Then $$ab = l^2, \quad \dot{a}^2-\dot{b}^2 = U^2, \tag{2.14}$$

so $$b = \frac{l^2}{a}, \quad \dot{b} = -\frac{l^2\dot{a}}{a^2}, \tag{2.15}$$

$$\dot{a}^2\left(1-\frac{l^4}{a^4}\right) = U^2, \tag{2.16}$$

hence $$Ut = \pm\int^a\left(1-\frac{l^2}{a^4}\right)^{\frac{1}{2}}da. \tag{2.17}$$

On the other hand we may have

Axisymmetric flow. This corresponds to

$$c = b, \tag{2.18}$$

so $$ab^2 = 2L^3, \quad \dot{a}^2-2\dot{b}^2 = U^2; \tag{2.19}$$

hence $$b = (2L^3)^{\frac{1}{2}}a^{-\frac{1}{2}}, \quad \dot{b} = -(\tfrac{1}{2}L^3)^{\frac{1}{2}}\dot{a}a^{-\frac{3}{2}} \tag{2.20}$$

and $$\dot{a}^2\left(1-\frac{L^3}{a^3}\right) = U^2; \tag{2.21}$$

hence $$Ut = \pm\int^a\left(1-\frac{L^3}{a^3}\right)^{\frac{1}{2}}da. \tag{2.22}$$

In both (2.17) and (2.22) the right-hand side is expressible as an elliptic integral.

It is noteworthy that, in the general case, a second surface $p = p_s(t)$ may be found from (2.5) and (2.6) provided that $p = p_s$ and $Dp/Dt = \dot{p}_s$ represent the same surface. The equation of the surface must clearly be

$$\frac{x^2}{a^2}-\frac{y^2}{b^2}-\frac{z^2}{c^2} = \frac{F+2p_s}{F} \tag{2.23}$$

from (2.5), and from (2.6) a similar equation with $(\dot{F}+2\dot{p}_s)/\dot{F}$ on the right. If we then take

$$p_s = \lambda F \tag{2.24}$$

with λ constant, the new surface is a hyperboloid similar to (2.10), and with semi-axes a', b', c' given by

$$\frac{a'}{a} = \frac{b'}{b} = \frac{c'}{c} = (1+2\lambda)^{\frac{1}{2}}. \tag{2.25}$$

3. The axisymmetric hyperboloid

The two-dimensional case (2.17) has already been discussed (with a different approach) by Longuet-Higgins (1972, 1976), showing, in particular, that the fluid accelerations become infinite when the angle between the asymptotes passes through 90°. We give now an analogous discussion for the axisymmetric case.

The free surface ($k = 0$) is given by

$$\frac{x^2}{a^2} - \frac{y^2+z^2}{b^2} = 1. \tag{3.1}$$

This represents a hyperboloid of two sheets, having the x-axis as axis of symmetry (see figure 2). A section by the plane $z = 0$ gives the hyperbola

$$\frac{x^2}{a^2} - \frac{y^2}{b^2} = 1. \tag{3.2}$$

To fix the ideas we shall discuss the lower branch, for which $x > 0$.

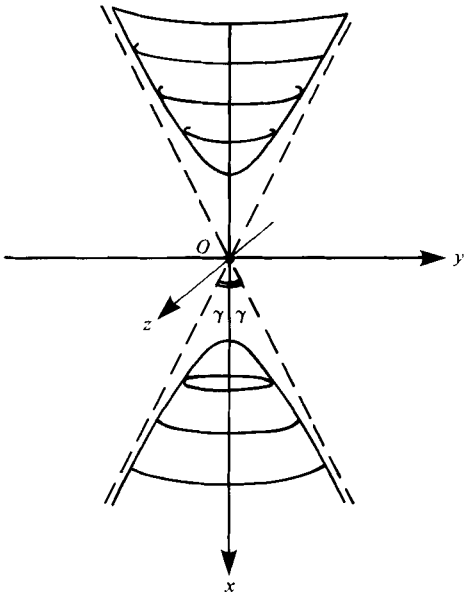

FIGURE 2. Axisymmetric hyperboloid corresponding to (3.1).

Introduce dimensionless variables

$$\alpha = \frac{a}{L}, \quad \beta = \frac{b}{L}, \quad \tau = \frac{Ut}{L}, \tag{3.3}$$

so that

$$\alpha\beta^2 = 2, \tag{3.4}$$

and (2.22) becomes

$$\tau = \int_1^\alpha (1-\alpha^{-3})^{\frac{1}{2}} d\alpha, \tag{3.5}$$

the lower limit being suitably chosen. The angle between the asymptotes is 2γ, where

$$\tan\gamma = \frac{b}{a} = \frac{\beta}{\alpha} = \frac{2^{\frac{1}{2}}}{\alpha^{\frac{3}{2}}} \tag{3.6}$$

by (3.4), and the radius of curvature R at the vertex $(x, y) = (a, 0)$ is given by

$$R = \frac{b^2}{a} = \frac{L\beta^2}{\alpha} = \frac{2L}{\alpha^2}. \tag{3.7}$$

The velocity of a particle at the vertex is $(\dot{a}, 0)$, where

$$\dot{a} = \frac{U}{(1-\alpha^{-3})^{\frac{1}{2}}}. \tag{3.8}$$

Lastly

$$F = -a\ddot{a} = -U^2\alpha\alpha_{\tau\tau} = \frac{\frac{3}{2}U^2\alpha^{-3}}{(1-\alpha^{-3})^2}. \tag{3.9}$$

Consider the limit of (3.5) as $\alpha \to \infty$. When $\alpha > 1$ we have

$$\tau = \int_1^\alpha (1-\tfrac{1}{2}\alpha^{-3}-\tfrac{1}{8}\alpha^{-6}-\dots)\,d\alpha, \tag{3.10}$$

and so writing

$$\tau_0 = \int_1^\infty [(1-\alpha^{-3})^{\frac{1}{2}}-1]\,d\alpha = -1{\cdot}2936 \tag{3.11}$$

we have

$$\tau-\tau_0 = \alpha+\tfrac{1}{4}\alpha^{-2}+\tfrac{1}{40}\alpha^{-5}+\dots \tag{3.12}$$

or

$$\alpha = (\tau-\tau_0)-\tfrac{1}{4}(\tau-\tau_0)^{-2}+\dots. \tag{3.13}$$

Hence

$$\tan\gamma \sim \frac{2^{\frac{1}{2}}}{(\tau-\tau_0)^{\frac{3}{2}}}[1+\tfrac{3}{8}(\tau-\tau_0)^{-3}] \tag{3.14}$$

and

$$R \sim \frac{2L}{(\tau-\tau_0)^2}[1+\tfrac{1}{2}(\tau-\tau_0)^{-3}]. \tag{3.15}$$

It can be shown that the limiting form of the surface is a paraboloid whose dimensions contract like t^{-2} about a point of similarity O lying on the axis of symmetry at one-quarter the distance from the vertex of the parabola to the focus. This limiting form is one of the self-similar flows discussed in Longuet-Higgins (1976, §3).

Consider on the other hand the limit as $\alpha \to 1$. Writing $\alpha = 1+\eta$, $\eta > 0$, and substituting in (3.5), we have

$$\tau = \int_0^\eta [1-(1+\eta)^{-3})]^{\frac{1}{2}}\,d\eta \sim \frac{2}{\sqrt{3}}\eta^{\frac{3}{2}}. \tag{3.16}$$

Hence

$$\alpha \sim 1+\left(\frac{\sqrt{3}}{2}\tau\right)^{\frac{2}{3}}, \tag{3.17}$$

and (3.6) and (3.7) give

$$\left.\begin{aligned} \tan\gamma &\sim 2^{\frac{1}{2}}\left[1-\frac{3}{2}\left(\frac{\sqrt{3}}{2}\tau\right)^{\frac{2}{3}}\right], \\ R &\sim 2^{\frac{2}{3}}L\left[1-2\left(\frac{\sqrt{3}}{2}\tau\right)^{\frac{2}{3}}\right]. \end{aligned}\right\} \tag{3.18}$$

Also,

$$\dot{a} \sim \frac{2^{\frac{1}{3}}}{3^{\frac{2}{3}}}U\tau^{-\frac{1}{3}}. \tag{3.19}$$

Thus as $t \to 0$ the velocities (represented by $\dot{a}$) tend to infinity like $t^{-\frac{1}{3}}$ and the accelerations (also the normal pressure gradient) tend to infinity like $t^{-\frac{4}{3}}$. Hence the motion starts with a weak 'jolt' or shock, just as in the well-known two-dimensional case (Longuet-Higgins 1972). Further discussion of this phenomenon is given in the appendix.

Equation (3.19) shows that the limiting angle between the asymptotes is

$$\lim 2\gamma = 2\arctan 2^{\frac{1}{2}} = 109{\cdot}47° \tag{3.20}$$

compared with 90°, or $2\arctan 1^{\frac{1}{2}}$, in the two-dimensional case.

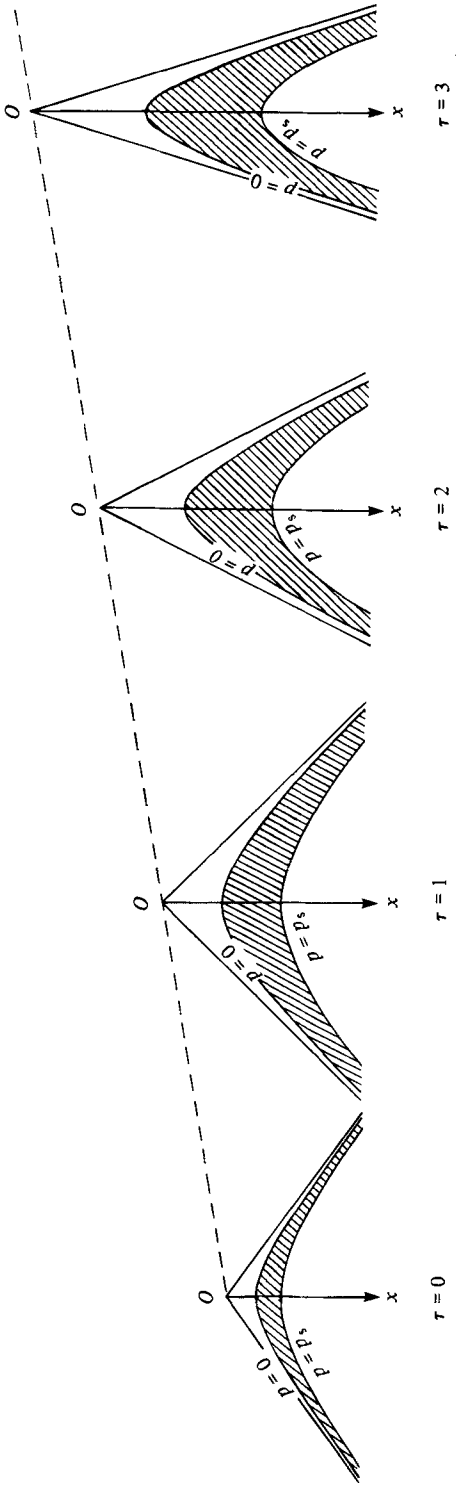

FIGURE 3. Time-development of an axial section of the hyperboloid $p = 0$ given by (3.2) with an additional free surface $p = \frac{3}{2}F$.

The function τ was calculated numerically by quadrature over the complete range $1 \leqslant \alpha < 10$. Representative values are given in table 1.

Figure 3 shows the development of the hyperbola as a function of the dimensionless time τ. For illustration we have shown not only the free surface $p = 0$, but also a second surface $p = p_s = \lambda F(t)$, with $\lambda = 1{\cdot}5$.

We note that values of α lying in the range $(0 < \alpha < 1)$ correspond to angles 2γ greater than (3.20). However, we then have $\dot{a}^2 < 2\dot{b}^2$ and U^2 would be negative. The normal pressure gradient at the free surface also changes sign, and there is reason to doubt that the flow is stable (cf. Longuet-Higgins 1972).

α	τ	2γ	R/l	F/U^2
1·00	0·0000	109·47°	2·0000	1·5000
1·04	0·0090	106·26°	1·8491	1·3335
1·16	0·0676	97·08°	1·4863	0·9610
1·36	0·2078	83·45°	1·0813	0·5963
1·64	0·4417	67·91°	0·7436	0·3401
2·00	0·7798	53·13°	0·5000	0·1875
2·44	1·1887	40·71°	0·3359	0·1033
2·96	1·6951	31·04°	0·2283	0·0578
3·56	2·2862	23·78°	0·1578	0·0332
4·24	2·9604	18·40°	0·1112	0·0197
5·00	3·7165	14·42°	0·0800	0·0120
5·84	4·5538	11·44°	0·0586	0·0075
6·76	5·4719	9·20°	0·0438	0·0049
7·76	6·4706	7·49°	0·0332	0·0032
8·84	7·5496	6·16°	0·0256	0·0022
10·00	8·7089	5·12°	0·0200	0·0015

TABLE 1. Values of τ, 2γ, R/L and F/U^2 as functions of α

4. Comparison with observation

To establish a coordinate system for figure 1 we chose two particular coordinate frames, numbers 50 and 80, in which the hyperbolic form of the jet was sufficiently clear, and inserted, in each case, the centre of the hyperbola at the intersection of the asymptotes. The frames being equally spaced in time, a straight line was drawn through these two points; the other centres, some of which were less clear, were assumed to lie on this line. From each centre, asymptotes were then drawn to the hyperbolic part of each profile. The angles 2γ between the asymptotes are shown in table 2.

Frame number	2γ	τ
30	104°	0
40	47°	1·125
50	24°	2·25
60	15°	3·375
70	10°	4·5
80	8·5°	5·625
90	7°	6·75
100	6·5°	12·6

TABLE 2. Measured values of the angle 2γ between the asymptotes in figure 1

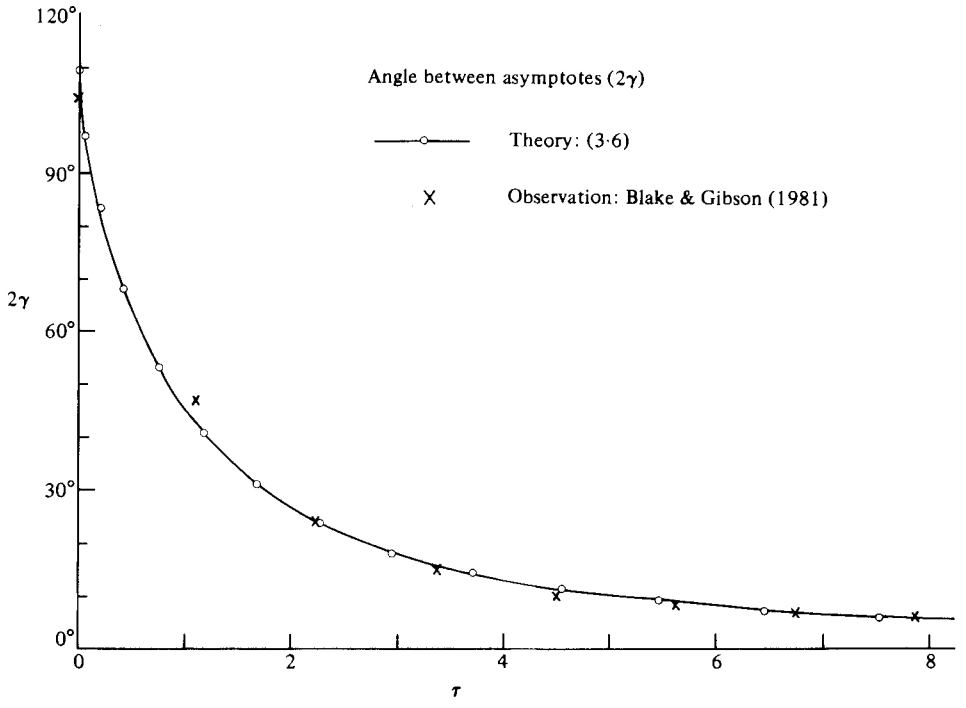

FIGURE 4. Time history of the angle 2γ between the asymptotes according to (3.6). The plotted points correspond to the observations in figure 1.

In theory, since the reference frame in §§2 and 3 above is inertial, i.e. in free fall, the trajectory of the centre C should actually be in a free-fall parabola. However, the elapsed time between frames 30 and 100 – 5·5 ms – is so short that the curvature of the trajectory is quite negligible: the maximum deflection would be about one part in 10^3.

To obtain a dimensionless time τ, it was noted that the angles 2γ corresponding to the two frame numbers 50 and 80 were 24° and 7°, corresponding to $\tau = 2{\cdot}25$ and 6·75 respectively. The values of τ for the other frames were then inferred by linear interpolation (and extrapolation) giving the numbers shown in column 3 of table 2. These have been plotted in figure 4. The agreement with the theoretical curve will be seen to be quite good. Especially notable is the observed angle 104° in frame no. 30, which is only a little less than the critical angle of 109·5°. It appears a coincidence that this was one of the frames selected for display.

In figure 10 of Blake & Gibson (1981) there was one further figure (10.11) corresponding to a frame number 142. Extrapolation gives for this frame $\tau = 12{\cdot}6$ and hence, from the model of §3, $2\gamma = 3{\cdot}6°$. The angle measured from the photograph is about 3°, so that the agreement is maintained even as far as this point.

Near the base of the jet in figure 1, where fluid is apparently being drawn into the hyperboloid, close agreement is not to be expected. In fact the photographs from frame 50 onwards show the formation of a smaller, reverse jet directed into the cavity, which by frame 100 has actually penetrated the lower cavity wall. Nevertheless, given the unplanned character of the initial conditions, it is remarkable that the form of the upwards jet should be so stable.

The downwards jet appears similar to that produced by a shaped charge (see Birkhoff *et al.* 1948). These authors model the phenomenon by a steady flow. Their observations, however, indicate a uniform rate of strain in the jets, more in accord with the present theory.

The asymmetrical collapse of cavitation bubbles in the interior of a fluid or near a solid surface has been discussed by Benjamin & Ellis (1966), Plesset & Chapman (1971) and many others. From the theory of §3 one would expect the maximum acceleration of the inwards jet to occur when the 'angle of indentation' of the bubble reached a critical value of around 109·5°. Such a result appears not inconsistent with the numerical calculations shown in figures 1 and 2 of Plesset & Chapman (1971), for example. However the development of an *inwards* jet is necessarily limited in time and space by the presence of the cavity walls, so that comparison with the ideal hyperbolic form is less feasible than for a bubble breaking a free surface.

Jets formed by a hollow liquid surface (without lining) have been produced artificially by Bowden (1966), and are probably quite a common phenomenon. They appear to be similar to the jets arising from the bowl of any small bubble (diameter 1–2 mm) bursting at a free surface (see Blanchard & Woodcock 1980; MacIntyre 1968, figure 1). Similar jets may model the 'splash' produced after a solid body has fallen rapidly through a free surface; see Worthington (1908).

5. Standing gravity waves

The observed tendency towards the formation of jets in cavitation or vapour bubbles prompts one to enquire whether a similar phenomenon may occur in other situations involving free-surface flows. One example of such a flow is a standing gravity wave, driven slightly beyond its maximum amplitude.

Already in the case of standing waves in two dimensions, it was suggested (Longuet-Higgins 1972) that the Dirichlet hyperbola, with a critical angle of 90°, might model some of the instabilities found experimentally by Taylor (1953) in standing waves of finite amplitude. It was verified recently by McIver & Peregrine (1981) that numerically calculated profiles of overdriven standing waves do indeed conform to the Dirichlet hyperbola.

Turning now to axisymmetric gravity waves of finite amplitude, we note that in a theoretical study Mack (1962) has suggested that a standing wave of maximum amplitude should have a critical interior angle of $2 \arctan \sqrt{2}$ at the crest – the same critical angle that was found above in §3. Mack's argument, which depends on the pressure p being expansible everywhere as a Taylor series, even at the crest of the wave, resembles the argument put forward by Penney & Price (1952) for a crest angle of 90° in two-dimensional standing gravity waves of limiting amplitude, and so is open to the same criticism as was directed against it by Taylor (1953), namely, there appears no conclusive reason for assuming that at the instant of maximum elevation there is not a singularity in the pressure p at the crest. Taylor nevertheless showed experimentally that the angle at the crest of a two-dimensional wave was close to 90°. We may wonder whether, just as the two-dimensional Dirichlet hyperbola describes an overdriven standing wave in two dimensions, so the axisymmetric Dirichlet hyperboloid may describe an overdriven axisymmetric standing wave.

Some controlled experiments on axisymmetric gravity waves of finite amplitude were undertaken by Fultz & Murty (1963; see also Edge & Walters 1964). These experiments tended to verify some of Mack's other theoretical results, but they were apparently not carried as far as waves of maximum amplitude. The reason no doubt

lay in the method of wave generation, which was by a plunger close to the free surface, on the axis of symmetry. This would tend to generate turbulence, and to interfere with the surface at the crest.

However, Faraday (1831) showed that standing waves could be generated in a layer of liquid on the surface of a vibrating plate, or by the vertical oscillation of a relatively deep vessel of liquid, and that the waves so produced were often of *half* the frequency of excitation. Physically, as we now know, this subharmonic resonance is related to the existence, in ordinary standing water waves, of pressure fluctuations at great depths having a frequency double the fundamental frequency of the wave (see Miche 1944; Longuet-Higgins & Ursell 1948). These second-order pressure fluctuations remain of finite amplitude, i.e. not tending to zero as one descends in the fluid, and they have been shown to be responsible for oceanic microseisms of double the frequency of the sea waves (Longuet-Higgins 1950; Haubrich, Munk & Snodgrass 1963). Conversely, one finds that, by creating widespread pressure fluctuations at great depths, standing surface waves of half the existing frequency can be produced.†

In §6 we shall describe an experiment in which this type of excitation is used to generate an upwards pointing jet.

6. Experiments on breaking waves

A cylindrical glass beaker of height 27 cm and internal diameter 16·4–16·5 cm was filled with water to a depth of 18·5 cm and placed on a horizontal wooden platform, attached to a Derritron vibrator (type VP4B) as in figure 5. The vibrator was driven by an electronic oscillator (Type 300WT, Mk 2) capable of producing sinusoidal vertical movements of amplitude 0·5 mm at frequencies from 0·5 to 1000 Hz.

In the centre of the beaker was placed a thin baffle, consisting of two mutually perpendicular sheets of aluminium, each of width 5·08 cm, mounted vertically on a brass base, the top of the baffle being about 6·0 cm below the water surface. The purpose of this was to damp out the lower asymmetric modes of oscillation, while leaving the axisymmetric modes relatively unhindered.

The oscillator was driven at a constant frequency $f_e = 6{\cdot}64$ Hz – slightly less than twice the calculated resonant frequency of 3·43 Hz for the lowest axisymmetric mode of free oscillation (including surface tension but disregarding viscous effects at the walls of the cylinder). As the amplitude of the oscillator was increased from zero to about 0·3 mm, there first appeared at the free surface synchronous surface oscillations with a fundamental frequency equal to the forcing frequency. These were axisymmetric, with radial modenumber 6. They then gave way to synchronous oscillations with azimuthal modenumber 4 or 6. Finally there was a dramatic transition to a subharmonic axisymmetric oscillation of half the driving frequency. With the amplitude of the vertical excitation set at about 0·3 mm the subharmonic axisymmetric mode could be maintained in a quasi-steady state indefinitely, with the silhouette of the free surface approaching a sharp corner of about 110°, as, for example, seen in figure 6(*a*). The slight rounding of the crest is due presumably to surface tension.

The attainment of this form was however very sensitive to the chosen frequency of excitation. At slightly lower frequencies f_e the subharmonic axisymmetric mode of frequency $\frac{1}{2}f_e$ itself became subject to subharmonic oscillations, axisymmetric or otherwise, notably with frequencies $\frac{1}{4}f_e$ or $\frac{1}{6}f_e$.

† For a mathematical analysis based on Matthieu functions see Benjamin & Ursell (1954).

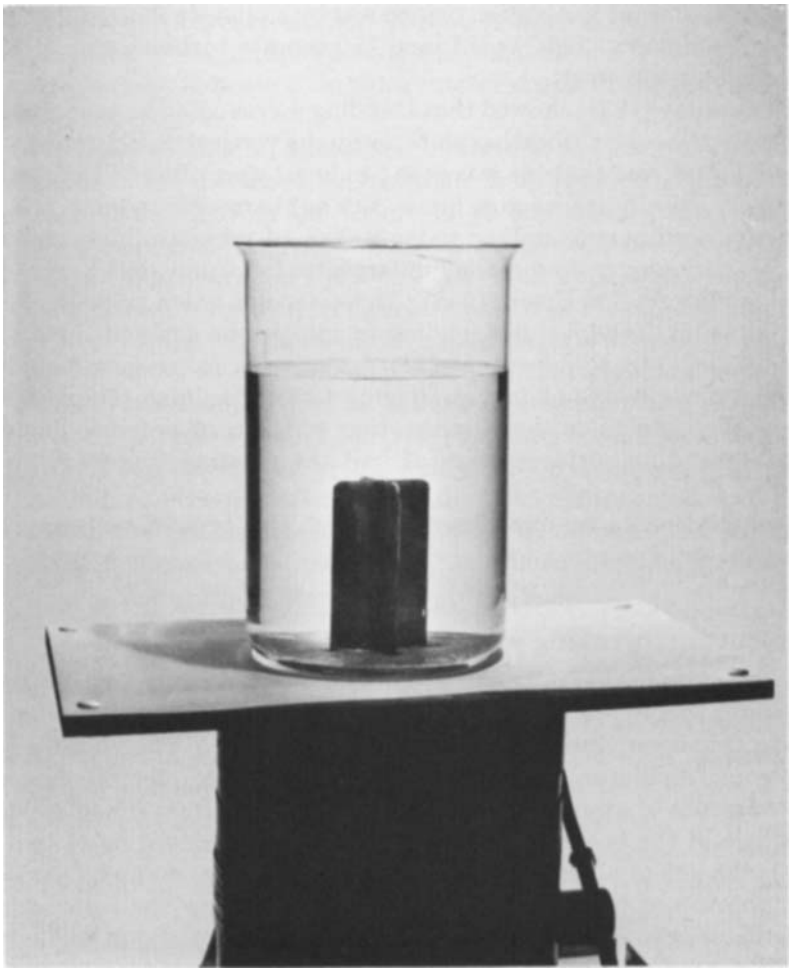

FIGURE 5. Glass beaker placed on a vertical Derritron vibrator, in a state of rest. The vertical flanges on the axis are to suppress asymmetric modes of oscillation.

When the axisymmetric oscillation was overdriven by increasing the amplitude of excitation to about 0·5 mm, the amplitude of oscillation quickly increased (see figures 6*b–c*) and the profile became unstable (figure 6*f*), ultimately producing an upwards jet along the vertical axis (figures 6*g*, 7). The most spectacular jets rose to a height of more than 170 cm above the free surface (i.e. ten times the diameter of the flask), as proved by splashes found at this height on the white cardboard background. These however were initiated on the axis of symmetry, near the instant when the free surface was at its *lowest* point; the standing wave had already degenerated so far that it somewhat resembled a collapsing bubble (see MacIntyre (1968, figure 1). The fact that the tip of the jet was well-formed (i.e. sharply pointed) by the time that it rose above the mean level meant that the time history of the angle could not be measured very accurately, at least in its early stages.

Nevertheless, the initial acceleration of some jets, which produced velocities of order 8 m/s in less than 0·05 s must have been in excess of 15*g*.

The conclusions from this experiment are, first, that steady axisymmetric standing waves can apparently be generated with a vertex angle *less* than the supposed critical

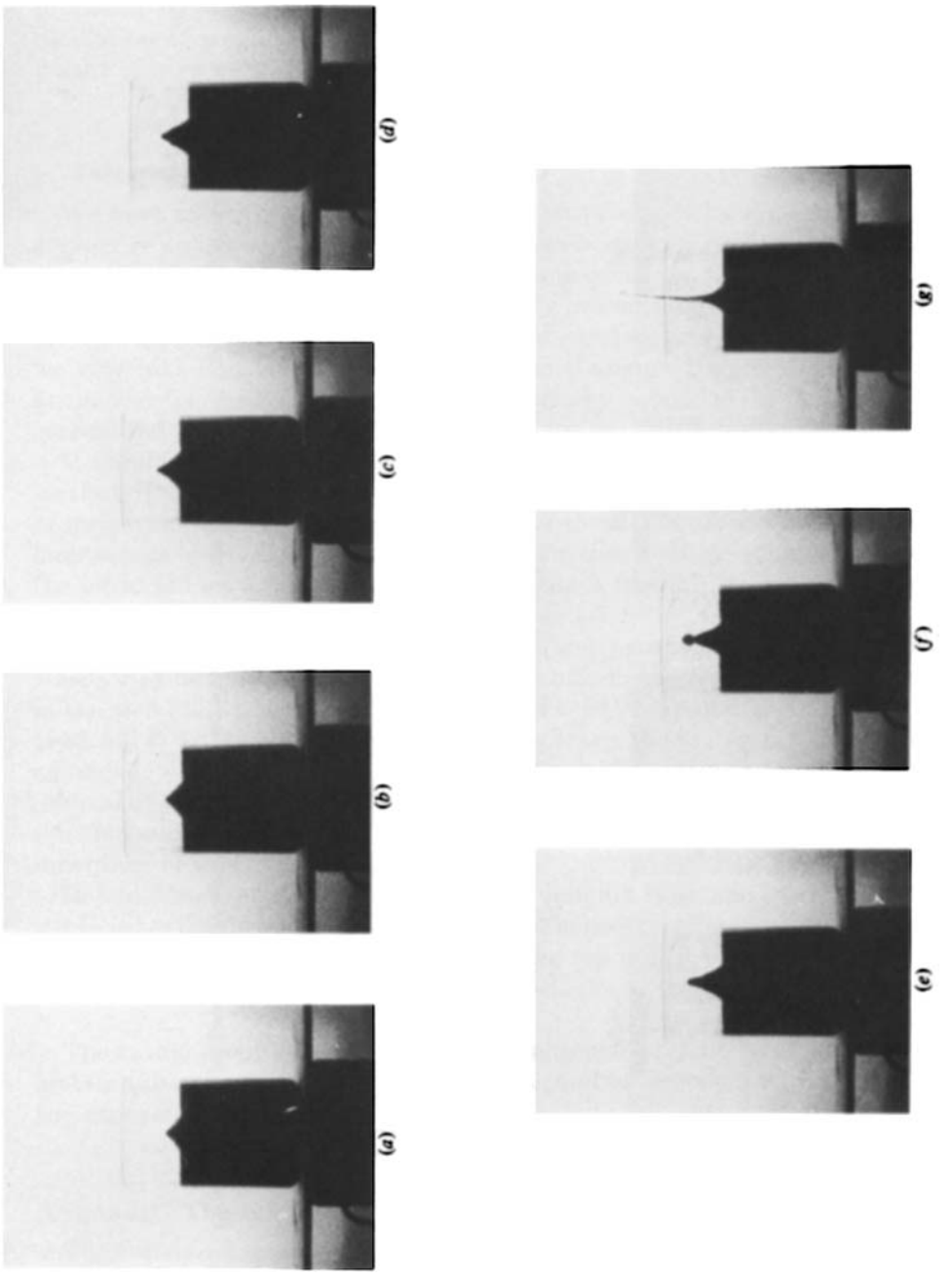

FIGURE 6. Crest profiles of successive standing waves (frequency approximately 3·43 Hz) excited subharmonically by a vertical oscillation (frequency 6·64 Hz). The interval between frames is about 0·29 s.

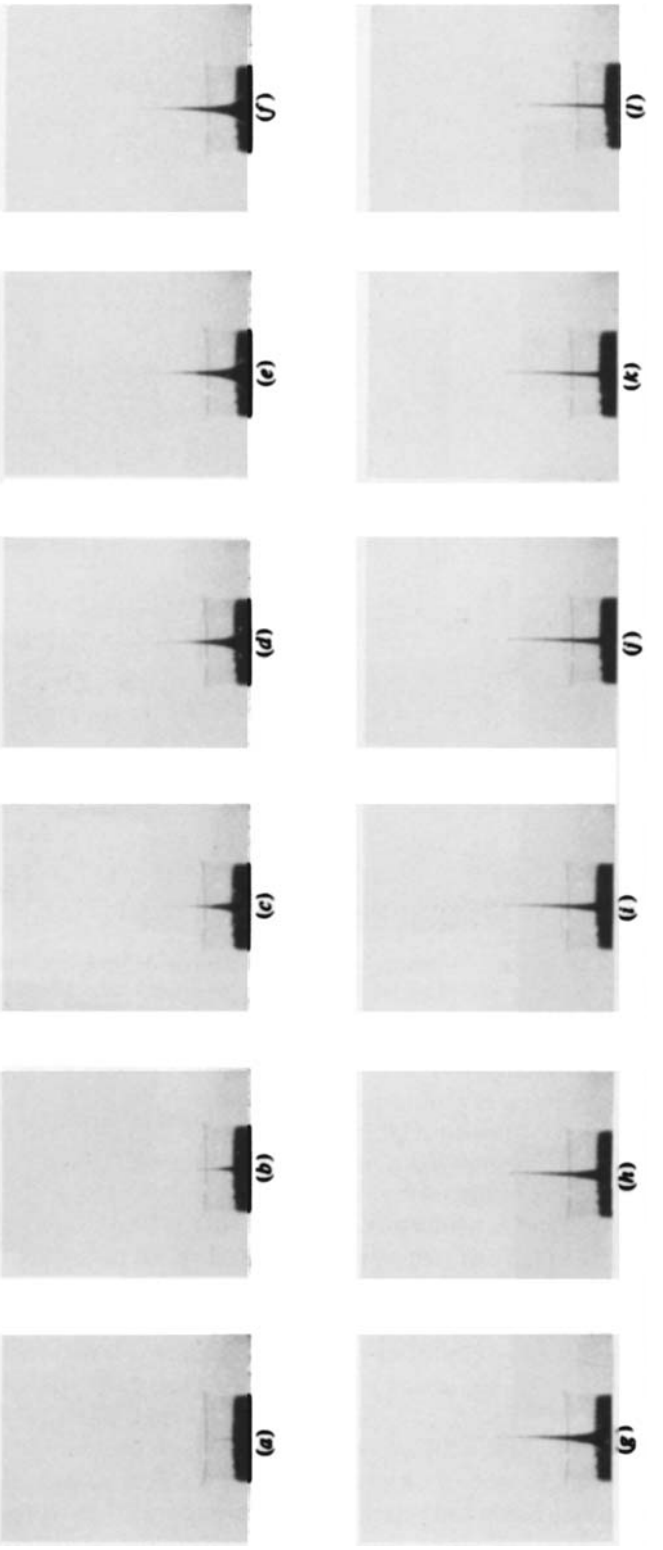

FIGURE 7. The jet produced by an overdriven standing wave. Time lapse between frames is approximately 0·01 s.

angle of 109·5°. Second, that by overdriving the waves an unsteady, axisymmetric jet, similar to that produced by an expanding gas bubble, can indeed be produced; and, third, that the jet originates not near the crest of the wave (where it might have been expected), but in the trough of the wave, in a similar way to the main splash produced by a small bursting bubble (MacIntyre 1968). The fact that a small oscillation of amplitude as little as 0·5 mm can ultimately produce a jet rising to a height of over 1·7 m must also be considered remarkable.

7. Discussion

We have shown that the axisymmetric jet produced by a gas bubble near a free surface is well modelled by the inertial, inviscid, hyperbolic flow described in §3. Moreover, a very similar jet has been shown to occur in axisymmetric standing waves driven beyond their limiting amplitude. By inference we may expect that such jets are a possible characteristic of other types of unsteady free-surface flow. In particular, we may take note of a previous suggestion (Longuet-Higgins 1980) that the tip of an *overturning* gravity wave may be suitably modelled by a hyperbolic jet of generalized form, in which the principal axes are in rotation.

It should be emphasized that the jets discussed in this paper are to a high degree inertial, that is independent of both gravity and surface tension. In the initial stages of formation, the time scale is too short for these other forces to exert an effect. At later stages both gravity and surface tension may become effective. Gravity causes the jet to fall back, and the origin to describe a free-fall trajectory. Surface tension can cause the jet to break up into droplets.

However, the evident stability of the jet under surface tension is remarkable. The reason may be that the flow is not simply a uniform inextensible stream, as is assumed in the well-known perturbation analysis of a jet of circular cross-section (see Lamb 1932, §274). In the hyperbolic jet, on the contrary, the free surface is constantly being extended, with the consequence that any wavelike perturbation of the flow is being drained of energy by the radiation stresses. Conversely, if time were reversed so that the free surface were being contracted, the flow would be highly unstable, quite regardless of surface tension.

In two-dimensional breaking waves of plunging type, the jet is continually being stretched in the direction of motion, but not in the transverse direction. One therefore expects instabilities to appear at first across the flow, with crests aligned parallel to the jet. This is what is commonly observed.

The author is indebted to John Blake for arousing his interest in cavitation bubbles and for subsequent stimulating discussions, and to Norman Smith for assistance with the experiments described in §6.

Appendix. The initial 'shock': a physical discussion

The outstanding feature of the flows described above is the occurrence of a singularity in both velocity and acceleration at the critical instant $t = 0$. What is the reason?

Consider first the two-dimensional flow (2.13) and choose the simplest case when the hyperbolic cross-section reduces to a pair of straight lines enclosing the variable angle 2γ, as in figure 8. It is useful to express the flow in Lagrangian coordinates in

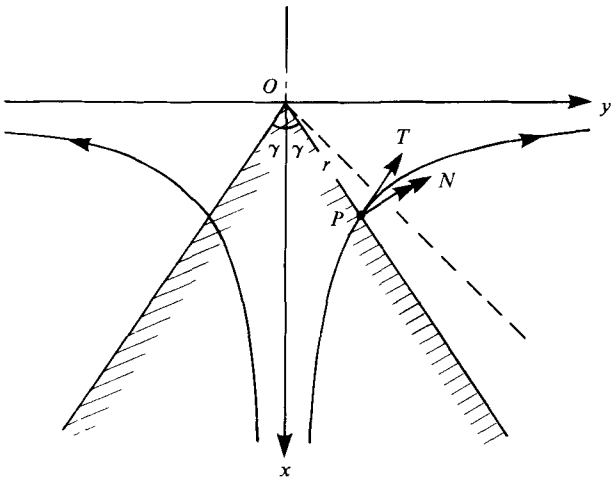

FIGURE 8. Illustration of the streamlines and the free surface in a two-dimensional wedge. (The vertex angle 2γ is shown increasing.)

which the position (x, y) of a particle is given as a function of t and the initial position (x_0, y_0) by

$$x = ax_0, \quad y = by_0. \tag{A 1}$$

Then the velocity $(\dot{x}, \dot{y})$ is $(\dot{a}x_0, \dot{b}y_0)$, satisfying (2.2). The equation of continuity yields

$$1 = \frac{\partial(x, y)}{\partial(x_0, y_0)} = ab, \tag{A 2}$$

as in (2.14), with $l = 1$. The particle trajectories are therefore rectangular hyperbolae given by

$$xy = x_0 y_0 = \text{constant} \tag{A 3}$$

(see figure 8).

On the other hand the pressure field, from the Lagrangian equations

$$\left.\begin{aligned} p_{x_0} &= -x_{x_0}\ddot{x} - y_{x_0}\ddot{y} = -a\ddot{a}, \\ p_{y_0} &= -x_{y_0}\ddot{x} - y_{y_0}\ddot{y} = -b\ddot{b}, \end{aligned}\right\} \tag{A 4}$$

is given by

$$p = -\tfrac{1}{2}(a\ddot{a}x_0^2 + b\ddot{b}y_0^2) + F(t). \tag{A 5}$$

By taking $F \equiv 0$ we ensure that the free surface ($p = 0$) consists of two straight lines through the origin, or alternatively that we are observing the flow out at infinity in the (x, y)-plane.

Consider then a particle $P(x, y)$ in the free surface, and to fix the ideas suppose the flow is reversed in time, so that the vertex angle 2γ is less than 90° and is *increasing*. The tangent PT to the trajectory makes an acute angle OPT with the vector PO. Moreover since the trajectory curves always to the right (i.e. clockwise) the angle OPT is increasing towards 90°. On the other hand, the only force accelerating the particle is the pressure gradient, which is in the direction of the normal PN to the free surface. If there were no force at all, the direction of the tangent to the trajectory would not vary. Clearly the only way OT can be made to curve towards the right by the purely normal pressure gradient is by making the normal component of velocity increase to infinity.

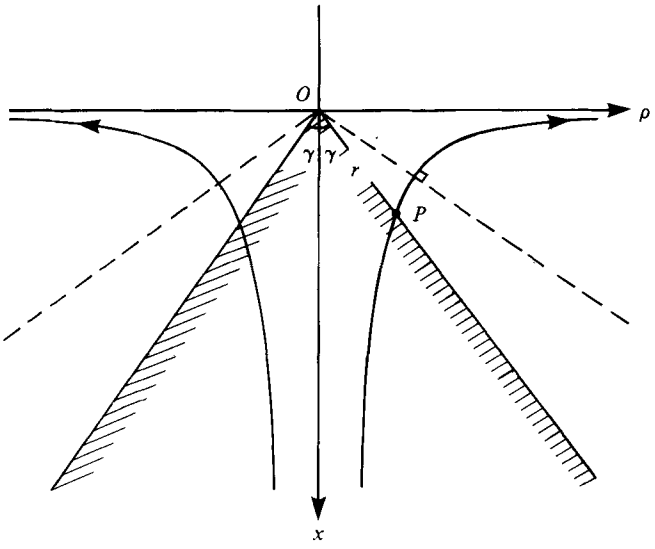

FIGURE 9. As in figure 8, but for an axisymmetric, or conical, flow.

A direct but very brief analytical proof is as follows. From (7.3) we have

$$\frac{\dot{x}}{x}+\frac{\dot{y}}{y}=0, \tag{A 6}$$

hence

$$\frac{\dot{x}}{x}=-\frac{\dot{y}}{y}=G, \tag{A 7}$$

say. Thus

$$\begin{aligned}\frac{d}{dt}(\dot{x}^2-\dot{y}^2) &= 2(\dot{x}\ddot{x}-\dot{y}\ddot{y})\\ &= 2G(x\ddot{x}+y\ddot{y})\\ &= 2Gr(\ddot{x}\cos\theta+\ddot{y}\sin\theta),\end{aligned} \tag{A 8}$$

where (r,θ) are polar coordinates in the plane. The expression in brackets on the right represents the radial acceleration, which vanishes identically. Hence $\dot{x}^2-\dot{y}^2$ is a positive constant. But, because of the symmetry of the trajectory about $\theta = 45°$, we see that when $x \to y$ then $\dot{x}^2$ tends to $\dot{y}^2$. These simultaneous requirements are possible only if $\dot{x}$ and $\dot{y}$ each tend to infinity. In other words, the velocity becomes infinite.

Turning again to the axisymmetric case we can give a very similar physical explanation. The essential difference is that in the axisymmetric case the trajectory of a given particle is no longer symmetric about a line through O inclined at 45° to the x-axis. Instead, the tangent to the trajectory becomes normal to the radius vector at a different angle $\gamma = \arctan\sqrt{2}$, as shown in figure 9.

A formal proof is as follows. If ρ denotes $(y^2+z^2)^{\frac{1}{2}}$, the equation of continuity now requires that each trajectory satisfy

$$x\rho^2 = x_0\rho_0^2 = \text{constant}, \tag{A 9}$$

hence

$$\frac{\dot{x}}{x}=-\frac{2\dot{\rho}}{\rho}=G, \tag{A 10}$$

say; therefore

$$\frac{d}{dt}(\dot{x}^2-2\dot{\rho}^2) = 2(\dot{x}\ddot{x}-2\dot{\rho}\ddot{\rho})$$
$$= 2G(x\ddot{x}+\rho\ddot{\rho})$$
$$= 2Gr(\ddot{x}\cos\theta+\ddot{\rho}\sin\theta), \qquad \text{(A 11)}$$

where (r, θ) are now polar coordinates in the (x, ρ)-plane. The right-hand side vanishes as before. Hence $\dot{x}^2-2\dot{\rho}^2$ is a constant, and each of $\dot{x}^2$ and $\dot{\rho}^2$ must become infinite when $\dot{x}^2 \to 2\dot{\rho}^2$, that is when $\rho^2 \to 2x^2$, by (A 10). The critical angle is therefore $2\arctan\sqrt{2}$.

REFERENCES

Benjamin, T. B. & Ellis, A. T. 1966 The collapse of cavitation bubbles and the pressures thereby produced against solid boundaries. *Phil. Trans. R. Soc. Lond.* A **260**, 221–240.

Benjamin, T. B. & Ursell, F. 1954 The stability of the plane free surface of a liquid in vertical periodic motion. *Proc. R. Soc. Lond.* A **225**, 505–515.

Birkhoff, G., MacDougall, D. P., Pugh, E. M. & Taylor, G. I. 1948 Explosives with lined cavities. *J. Appl. Phys.* **19**, 563–582.

Blake, J. R. & Gibson, D. C. 1981 Growth and collapse of a vapour cavity near a free surface. *J. Fluid Mech.* **111**, 123–140.

Blanchard, D. C. & Woodcock, A. H. 1980 The production, concentration and vertical distribution of the sea-salt aerosol. *Ann. New York Acad. Sci.* **338**, 330–347.

Bowden, F. P. 1966 The formation of microjets in liquids under the influence of impact or shock. *Phil. Trans. R. Soc. Lond.* A **260**, 94–95.

Dirichlet, P. L. 1860 Untersuchungen über ein Problem der Hydrodynamik. *Abh. Kön. Ges. Wiss. Göttingen* **8**, 3–42.

Edge, R. D. & Walters, G. 1964 Period of standing gravity waves of largest amplitude on water. *J. Geophys. Res.* **69**, 1674–1675.

Faraday, M. 1831 On a peculiar class of acoustical figures, and on certain forms assumed by groups of particles on vibrating elastic surfaces. *Phil. Trans. R. Soc. Lond.*, pp. 299–340.

Fultz, D. & Murty, T. S. 1963 Experiments on the frequency of finite-amplitude axisymmetric gravity waves in a circular cylinder. *J. Geophys. Res.* **68**, 1457–1462.

Haubrich, R. A., Munk, W. H. & Snodgrass, F. E. 1963 Comparative spectra of microseisms and swell. *Bull. Seism. Soc. Am.* **53**, 27–38.

Lamb, H. 1932 *Introduction to Hydrodynamics.* 6th edn. Cambridge University Press.

Longuet-Higgins, M. S. 1950 A theory of the origin of microseisms. *Phil. Trans. R. Soc. Lond.* A **243**, 1–35.

Longuet-Higgins, M. S. 1972 A class of exact, time-dependent, free-surface flows. *J. Fluid Mech.* **55**, 529–543.

Longuet-Higgins, M. S. 1976 Self-similar, time-dependent flows with a free surface. *J. Fluid Mech.* **73**, 603–620.

Longuet-Higgins, M. S. 1980 On the forming of sharp corners at a free surface. *Proc. R. Soc. Lond.* A **371**, 453–478.

Longuet-Higgins, M. S. 1983 Rotating hyperbolic flow: particle trajectories and parametric representation. *Q. J. Mech. Appl. Math.* **36** (May 1983).

Longuet-Higgins, M. S. & Ursell, F. 1948 Sea waves and microseisms. *Nature* **162**, 700.

MacIntyre, F. 1968 Bubbles: a boundary-layer 'microtome' for micron-thick samples of a liquid surface. *J. Phys. Chem.* **72**, 589–592.

McIver, P. & Peregrine, D. H. 1981 Comparison of numerical and analytical results for waves that are starting to break. In *Proc. Symp. on Hydrodynamics in Ocean Engineering, Trondheim, Norway, August* 1981, pp. 203–215. University of Trondheim.

Mack, L. R. 1962 Periodic, finite-amplitude, axisymmetric gravity waves. *J. Geophys. Res.* **67**, 829–843.

MICHE, R. 1944 Mouvements ondulatoires de la mer en profondeur constante ou décroissante. *Ann. Ponts et Chaussées* **114**, 27–78, 131–164, 270–292, 369–406.

PENNEY, W. G. & PRICE, A. T. 1952 Finite periodic stationary gravity waves in a perfect fluid. *Phil. Trans. R. Soc. Lond.* A **244**, 254–284.

PLESSET, M. S. & CHAPMAN, R. B. 1971 Collapse of an initially spherical vapour cavity in the neighbourhood of a solid boundary. *J. Fluid Mech.* **47**, 283–290.

TAYLOR, G. I. 1953 An experimental study of standing waves. *Proc. R. Soc. Lond.* A **218**, 44–59.

WORTHINGTON, A. M. 1908 *A Study of Splashes.* Longmans, Green & Co.